FLIGHT DEMONSTRATION OF A LONG RANGE ONBOARD DOPPLER LIDAR

Hamaki Inokuchi*, Tomohiro Akiyama*, and Katsuto Sasaki*
***Japan Aerospace Exploration Agency**

Keywords: *Flight Safety, Aviation Accident, Air Turbulence, Onboard Sensor, Flight Testing*

Abstract

Air turbulence is a major cause of aircraft accidents. Because of this, the JAXA (Japan Aerospace Exploration Agency) is developing an onboard turbulence detection system using a coherent Doppler LIDAR (Light Detection and Ranging) remote wind sensor that is small and light enough to be installed on an aircraft. The system will introduce two main technical advances to prevent turbulence-induced in-flight accidents: gust alleviation control to reduce lurching and providing pilots with turbulence information while cruising or changing altitude and turbulence encounter warning during landing approach. This paper describes flight test evaluation of the maximum observation range and measurement accuracy of the Doppler LIDAR for pilot information provision.

1 Introduction

Accident investigation reports of the Japan Transport Safety Board reveal air turbulence to be a major causal factor in aircraft accidents [1], contributing to about half of accidents to large aircraft in Japan. Although it is possible to avoid cumulonimbus clouds with intense turbulence as they can be detected by onboard radar, it is currently not possible for aircraft to detect clear air turbulence (that is, turbulence without clouds) before encountering it. For this reason, JAXA is researching and developing a Doppler LIDAR sensor capable of remotely detecting turbulence in largely clear air conditions [2, 3, 4, 5], and conducted the SafeAvio project [6] aimed at the flight demonstration of the system that includes providing information to pilots.

In the project reported in this paper, we developed a compact, high-performance Doppler LIDAR [7] as a turbulence detection sensor. Based on the sensor information of airflow ahead of the aircraft, a flight demonstration was carried out with the aim of providing information to support pilot decision-making on whether to execute a go-around due to turbulence encountered during landing approach [8], and on whether to switch on seat belt signs during cruise and altitude changes. Flight experiments also evaluated the Doppler LIDAR's maximum observation range and wind speed measurement accuracy. Gust alleviation control [9] was out of the project scope.

The flight demonstration was carried out as a series of 19 flights over the land and sea around the Chubu area of central Japan between December 17, 2016 and February 10, 2017.

2 Turbulence Detection System

The main components of the developed Doppler LIDAR turbulence detection sensor are shown in Fig. 1, and the sensor's main specifications are shown in Table 1. Laser pulses generated by an optical transceiver are amplified by optical amplifiers [10] incorporated in an optical antenna and radiated into the atmosphere from optical telescopes. The heat generated by the optical amplifiers is dissipated by a chiller unit using water as a coolant. The optical antenna was equipped with a 150-mm large aperture telescope for long range observations and a 50-mm small aperture telescope for vector conversion of short range wind velocities.

Fig. 1. Developed Doppler LIDAR wind sensor.

Table 1. Specifications of the LIDAR.

Laser Wavelength	1.55 μm
Laser Output	3.3 W
Pulse Repetition Frequency	1,000 Hz
Laser Beam Diameter	150, 50 mm
System Weight	83.7 kg
Electric Consumption	936 W

Emitted laser light is scattered by fine aerosol particles present in the atmosphere, and some is reflected back towards the transmitter. The backscattered light is condensed by the optical telescopes and received by an optical transceiver.

A signal processing unit control the system and processes the received light signals to obtain wind speeds at different distances. Since the wavelength of the received light is shifted by the Doppler effect according to the motion of the aerosol particles, the speed of the aerosol particles, and thereby the wind speed, can be obtained by comparing the wavelength of the received light with that of the transmitted light. At the same time, by sampling the received light signal corresponding to a transmitted pulse over a range of time intervals, it is possible to independently obtain the wind speed at different observation ranges corresponding to the round-trip time of the light.

The weight of the signal processing unit is not included in Table 1 as the prototype system uses an off-the-shelf general-purpose computer whereas a production model would use a custom avionics unit. The same applies to the keyboard and the display attached to the signal processor. However, the signal processor's electrical power consumption is included in the specifications as it is assumed that the power consumption of a production system would be about the same.

Doppler LIDAR is already applied for air flow observation in ground-based equipment and is used at some major airports. In comparison to such ground-based LIDARs, the airborne Doppler LIDAR sensor developed for this project has a higher maximum laser power output for high altitude wind measurement, since aerosol density is lower at altitude than at ground level, and its weight is about an order of magnitude lower.

For the flight demonstration, the optical antenna was mounted near the bottom of the forward pressure bulkhead inside the radome of a business jet aircraft so that the laser beam was emitted forward from the aircraft. A double wedge prism-type scanner was installed in front of the laser radiation part of the optical antenna so that the beam direction could be controlled from within the cabin and aligned with the direction of flight. All other system components were installed in the cabin.

3 Aerosol Measurement Unit

The maximum wind speed observation range of the LIDAR depends on the state of the atmosphere, particularly on aerosol density. Aerosol density changes with altitude and also depends on weather conditions [11]. For this reason, in the flight demonstration, Doppler LIDAR observations were made in horizontal flight at various altitudes while aerosol density was measured.

A block diagram of the atmospheric aerosol measurement unit is shown in Fig. 2. Atmospheric air is drawn from outside the aircraft through an inlet probe by a pump and aerosol density is measured by an OPC (Optical Particle Counter). During measurements, the aircraft maintained horizontal flight at a pitch angle of 2.5 degrees.

Aerosol density measurement requires compensation since atmospheric pressure decreases with altitude and the flow rate through the OPC will vary. To properly measure aerosol density regardless of altitude (airspeed, atmospheric pressure), the pump speed was controlled according to pressure altitude to maintain a flow rate through OPC equal to the aircraft's true airspeed (TAS), which achieves isokinetic sampling [12]. Although the TAS during measurements was 125 m/s near the ground, the air suction pressure was increased with altitude as the air density decreased and the airspeed increased correspondingly.

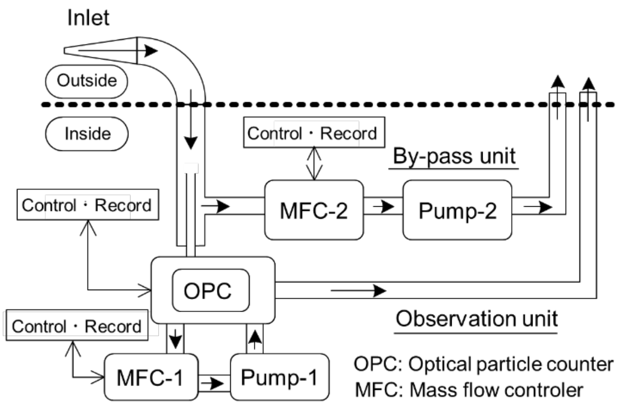

Fig. 2. Schematic Diagram of Atmospheric Aerosol Measurement Unit.

The inlet probe was designed with a 2 mm effective aperture diameter and a cone shape with a taper angle of 3.45 degrees to decelerate the atmospheric air entering the probe. As a result, the Reynolds number inside the pipeline was 1,800 or less regardless of flight altitude. Fig. 3 shows the appearance of the inlet probe mounted on the aircraft.

Fig. 3. Inlet Probe Mounted on the Aircraft.

4 Maximum Observation Range

In order to evaluate the maximum observation range of the sensor, a criterion is needed to judge to what extent observation is possible. In this project, the criterion was set by considering continuity of data.

An example of a received signal is shown in Fig. 4. The *y*-axis of the graph indicates the strength of the signal. The part shown by the ellipse on the left is the true signal, On the other hand, the part indicated by the right ellipse is noise, but because it is stronger than the true signal, it is recognized as a valid wind speed. This is a false detection. Since if the atmosphere is calm, the wind speed in an observed region of the atmosphere will scarcely change between successive measurements, it can be determined whether an apparent signal is true or false by confirming whether it is present in the same region of the atmosphere at a later time.

Noise is random and can occur anywhere within in the range of observation distances. Therefore, when a certain threshold value is set and the same wind speed is measured successively several times in almost the same region of the atmosphere, we determine that the sensor can make correct measurements up to the distance of that region; that is, we determine the observation range of the sensor.

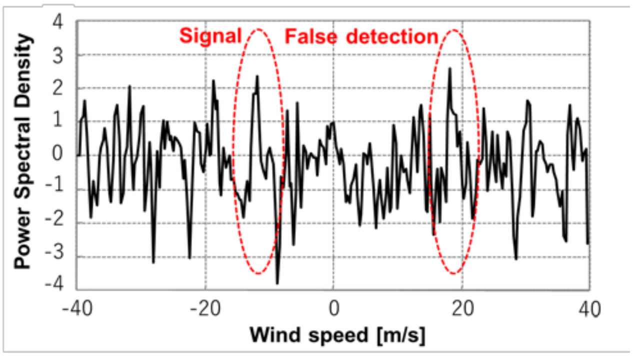

Fig. 4. Detected Signal Showing True and False Detections.

An example of calculating the maximum observation range with actual observation data values is shown in Fig. 5. The observation distance extending in the front of the aircraft was divided into 300 m range bins, and the numerical value within each frame in a vertical column in the table indicates the wind speed in the corresponding range bin at an observation time. Since the measurement range of the wind speed is ± 40 m/s as shown in Fig. 4, Fig. 5 shows values offset by the TAS so as not to exceed the measurement range. In the example of Fig. 5, the offset value is180 m/s is set, and the offset plus the numerical values in the cells in the figure indicate the relative speed between the aircraft and the atmosphere at a given distance and time.

In order to judge whether an observed wind speed is from the farthest valid measurement range bin, the wind speeds in approaching observation regions (bins) are evaluated over successive observations at one-second intervals. If the wind speed in a region of the atmosphere varies by less than ±1 m/s over four consecutive observations, then this measurement is considered as being valid. (Note that the bin corresponding to this region will change as the aircraft approaches it.) The furthest distance for which is true is determined to be the maximum observation range (the cyan boxes in Fig. 5), and range bins up to that distance also contain valid data (light blue in Fig. 5).

Although there may be data values that seem correct even at greater distances than the maximum observation range determined by this process, and there may be seemingly anomalous data values even at closer distances, the number of consecutive times was set to four considering the distance dependency and variance of the Signal-to-Noise Ratio (SNR), and the fact that no significant deviations from the SNR distribution were confirmed. The reason for the selection of ±1 m/s as the wind speed change threshold value is because this value is slightly greater than the turbulence detection system's accuracy requirement of ± 0.9 m/s so that correct data are not erroneously excluded.

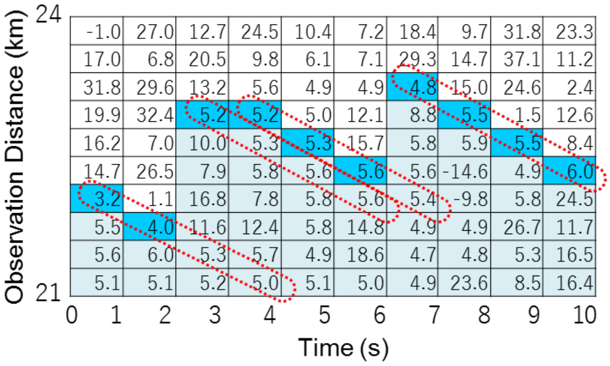

-1.0	27.0	12.7	24.5	10.4	7.2	18.4	9.7	31.8	23.3
17.0	6.8	20.5	9.8	6.1	7.1	29.3	14.7	37.1	11.2
31.8	29.6	13.2	5.6	4.9	4.9	4.8	15.0	24.6	2.4
19.9	32.4	5.2	5.2	5.0	12.1	8.8	5.5	1.5	12.6
16.2	7.0	10.0	5.3	5.3	15.7	5.8	5.9	5.5	8.4
14.7	26.5	7.9	5.8	5.6	5.6	5.6	-14.6	4.9	6.0
3.2	1.1	16.8	7.8	5.8	5.6	5.4	-9.8	5.8	24.5
5.5	4.0	11.6	12.4	5.8	14.8	4.9	4.9	26.7	11.7
5.6	6.0	5.3	5.7	4.9	18.6	4.7	4.8	5.3	16.5
5.1	5.1	5.2	5.0	5.1	5.0	4.9	23.6	8.5	16.4

Fig. 5. Calculated Maximum Observation Range

The test results of the maximum observation range at each altitude are shown in Fig. 6. The dashed blue line indicates the maximum observation range of the wind speed observed by the Doppler LIDAR and the solid green line indicates the aerosol density of particles 0.3 μm or more in diameter measured by the OPC by isokinetic sampling. Since the variation of the measurements was large, data were averaged over 7 to 10 observations Average values are plotted in Fig, 6 and standard deviations are shown by error bars. As altitude increases, aerosol density decreases and the maximum observation range tends to decrease correspondingly. However, the observation range at altitudes around 3,000 m was lower than expected from the aerosol density. The reason is presumed to be related to weather conditions; during the test flights, clouds frequently occurred around 3,000 m in the test area, and it is possible that core aerosol particles dropped with rain.

These results indicate that the sensor range can be over 20 km at low altitudes below 1,500 m. Since pilots can elect to go-around during a landing approach without air traffic control clearance, this range is considered to be sufficient to allow the sensor to indicate turbulence on the approach path and for the system to be used for go-around judgment. On the other hand, at high altitudes above 3,000 m, the average maximum observation range is about 10 km, which can only provide an advance warning of turbulence encounter of a few tens of seconds. Although such a warning makes it possible at least for seatbelt signs to be turned on, its effectiveness for accident prevention is likely to be limited.

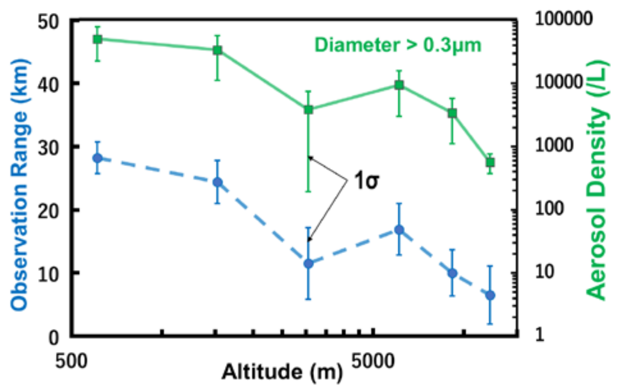

Fig. 6. Maximum Observation Range and Aerosol Density vs. Altitude.

5 Accuracy of Wind Speed Measurement

The wind speed observed by the Doppler LIDAR is the relative speed between the aircraft and the atmosphere and is equivalent to the TAS as long as air conditions remain calm. The TAS measured by the Doppler LIDAR sensor was therefore compared to the value of TAS computed from Pitot tube measurements and the TAS estimated value by the speed-course method under the calm air conditions to assess its accuracy.

As a result, it was found that the Doppler LIDAR can independently obtain TAS relative to the wind at each observation range, as shown in the example in Fig. 7.

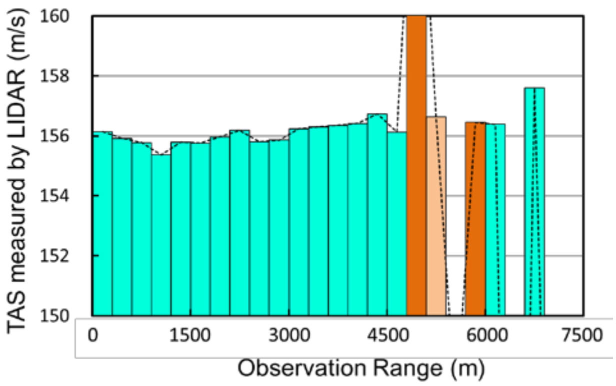

Fig. 7. LIDAR Detected True Airspeed and Observation Range.

The color of the bar graph indicates the SNR of the received signal: green (9 dB or more) shows where measurement with high reliability is possible. The deeper the orange color is, the lower the SNR and the measurement reliability. In this test case, at ranges below 4,800 m the observation reliability is high and the standard deviation in each range bin is 0.33 m/s, so it can be said that the atmosphere was relatively quiet during this flight. In fact, only few bumps due to turbulence were experienced during the flight. In this evaluation, an observation range of 300 to 600 m was used for measuring TAS by the Doppler LIDAR, because it may be impossible to obtain valid data at a very short distances and there is a possibility that the wind speed at a very long ranges may differ significantly from the local wind speed.

The speed-course method is a type of true airspeed (TAS) method that was used in the flight test to measure the position error of the air data sensor. The concept of the speed-course method is shown in Fig. 8. The influence of steady wind is eliminated by making a round-trip flight between two points at a constant altitude and speed. The method calibrates the air data sensor based on the inertial velocity, and the error (E) can be obtained by the following equation.

$$E = (V_{G1} - V_{M1} + V_{G2} - V_{M2}) / 2 \qquad (1)$$

The conditions under which the speed-course method is established are as follows.

① Steady wind conditions with only a horizontal component are used, and in this case the ground speed differences between the outbound and inbound legs of the round-trip flight due to the steady wind cancel each other out.

② Even if the measured speeds during the out and return legs are slightly different, the error E is assumed to be constant since V_{M1} and V_{M2} are almost the same.

When there is ground undulation or the altitude is increased, condition ① tends to collapse, so the error estimation accuracy generally deteriorates.

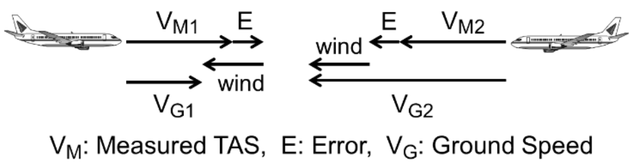

Fig. 8. The Speed-Course Method for Estimating Error in Airspeed.

The speed-course method was carried out at altitudes of 600 m, 3,000 m and 6,000 m, and the estimated value of TAS was obtained by adding the estimated error to the TAS measured by the Doppler LIDAR. The ground speed was obtained from a hybrid GPS/INS navigation system on the aircraft. The result is shown in Fig. 9. A bias-like difference is observed between the TAS measured by the Doppler LIDAR and the TAS computed from Pitot tube measurements. The average of the differences was 3.2 m/s, and the standard deviation excluding the difference was 0.22 m/s. Bias error is not so significant for turbulence measurement since wind speed differences rather than absolute speeds are of interest. Also, according to airworthiness standards, the error of the airspeed indicator is specified to be 3% or less, and the bias error and variation measured in this test can be said to be within the allowable range of the instrument.

Next, comparing the Doppler LIDAR with the speed-course method estimates, the speed-course method TAS values are close to those of the Doppler LIDAR at altitudes of 600 m and 3000 m, but at 6,000 m the speed-course TAS value is closer to the value derived from Pitot tube measurements. Considering that there is a possibility that the error of the speed-course method may become large at a high altitude, it is estimated that the accuracy of the TAS measurement by the Doppler LIDAR is equal to or higher than that obtained from Pitot tube measurements.

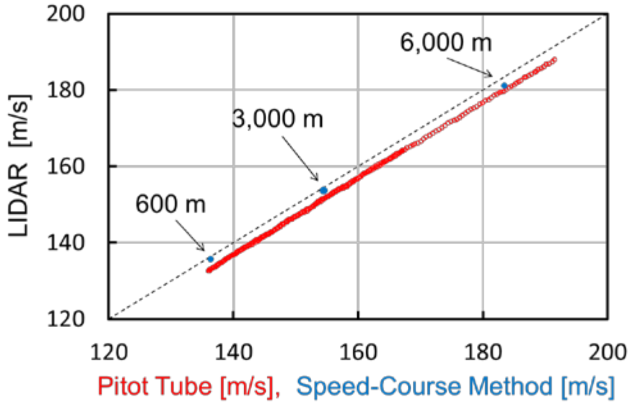

Fig. 9. Comparison of Measured Airspeeds.

6 Aerosol Density and LIDAR Signal Level

This section shows the relationship between the aerosol density and maximum observation range R of the LIDAR measured at around the same time.

Assuming that atmospheric transmittance is approximately 1 for simplicity, the SNR of the LIDAR received signal is proportional to 1 / R^2, where R is the observation range. When the SNR reaches a predetermined threshold value, the corresponding R is determined to be the maximum observation range. Fig. 10 shows measured aerosol densities and the maximum observation range R^2. For each aerosol density measurement, the average value of observation range obtained at a constant altitude for three minutes was used.

It is confirmed from Fig. 10 that there is a correlation between aerosol density and R^2, albeit with large variations. This is probably because (1) the LIDAR observation point is several kilometers to several tens of kilometers in front of the aircraft, whereas the aerosol density measurement is performed at the aircraft location, and (2) the direction of the LIDAR observation is tilted upwards and downwards when the aircraft's flight path is disturbed by, for example, light turbulence.

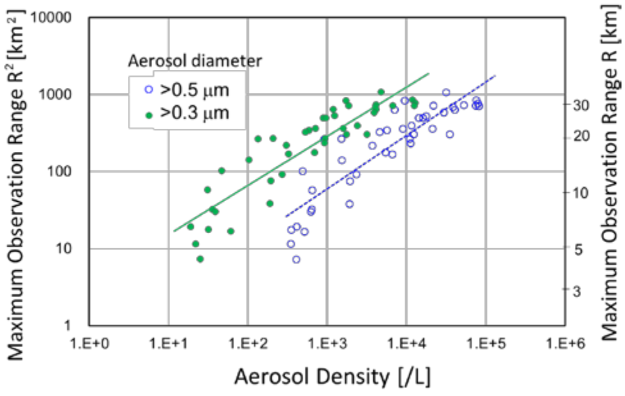

Fig. 10. Maximum Observation Range vs. Aerosol Density.

7 Concluding Remarks

With the implementation of the SafeAvio project, the following results were obtained for the turbulence detection system.

- A Doppler LIDAR remote wind sensor was developed as an aircraft on-board turbulence detection system that achieves high laser output power while being small and lightweight. A maximum observation range of greater than 20 km at low altitudes of 1,500 m or less was demonstrated in flight experiments, which is sufficient range for the sensor to be used to support pilot go-around judgment during landing approach. On the other hand, at high altitudes of 3,000 m or more the observation range is about 10 km on average, meaning that the system can only provide warnings of turbulence a few tens of seconds ahead. Although it is possible to turn on seat belt signs in this time, the effectiveness for accident prevention is limited.

- The wind speed measurement accuracy of the sensor was estimated from flight experiments to be equal to or higher than Pitot tube measurements, and the standard deviation was 0.22 m/s. For turbulence detection, the standard deviation is more important than absolute accuracy.
- The Doppler LIDAR sensor and an optical particle counter were installed on a business jet aircraft in order to carry out simultaneous measurements of wind speed and aerosol density. We were able to obtain data on aerosol density distribution as a function of altitude. We confirmed that the maximum observation range is affected by aerosol density, and that there is a positive correlation between the two.

In order to effectively prevent accidents at high altitudes, we will continue conducting research and development on a function to measuring the wind speed vector at short distances and gust alleviation of the aircraft by using measured turbulence speeds in feed forward control.

8 Contact Author Email Address

mailto:inokuchi.hamaki@jaxa.jp

References

[1] Japan Transport Safety Board, Aircraft accident reports, http://www.mlit.go.jp/jtsb/.

[2] Inokuchi H, Asaka K, and Hirano Y. Research and Development of an Onboard Wind Measurement LIDAR. *Abstracts of the Fourth Asian-Pacific Conference on Aerospace Technology and Science*, Chongqing, China, pp. 129-130, 2002.

[3] Inokuchi H, Tanaka H, and Ando T. Development of an Onboard Doppler LIDAR for Flight Safety. *Journal of Aircraft*, Vol. 46, No. 4, pp. 1411-1415, 2009.

[4] Inokuchi H, Tanaka H, and Ando T. Development of a Long Range Airborne Doppler LIDAR. *Proc 27th International Congress of the Aeronautical Sciences*, Nice, France, 10.4.3, 2010.

[5] Inokuchi H. Detection of the Clear Air Turbulence by an Airborne Doppler LIDAR. *Proc Asia-Pacific International Symposium on Aerospace Technology*, Jeju, Korea, 6.4.2, 2012.

[6] Machida S. *Project Overview of R&D for Onboard Turbulence Detection System*. Proc APISAT 2017, Seoul, Korea, Plenary Lecture 4, 2017.

[7] Inokuchi H, Akiyama T, and Machida S. *Development of an Onboard Safety Avionics System using a Doppler Lidar*. Proc 18th Coherent Laser Radar Conference, Boulder, USA, 2016.

[8] Iijima T, Uemura T, Matayoshi N, Entzinger J O, Matsumoto J, Ueda S and Yoshikawa E. *Development and Evaluation of a New Airspeed Information System utilizing Airborne Doppler Lidar*. 36th Digital Avionics Systems Conference, St. Peters berg, U.S.A, 2017.

[9] Hamada Y. *Aircraft Gust Alleviation using Discrete-Time Preview Controller with Prior Gust Information.* Proc SICE Annual Conference 2013, pp.1907-1912, Nagoya, Japan, 2013.

[10] Sakimura T, Watanabe Y, Ando T, Kameyama S, Asaka K, Tanaka H, Yanagisawa T, Hirano Y, Inokuchi H. *3.2 mJ, 1.5 μm laser power amplifier using an Er, Yb:glass planar waveguide for a coherent Doppler LIDAR. Proc 17th Coherent Laser Radar Conference*, Barcelona, Spain, 2013.

[11] Inokuchi H, Furuta M, Inagaki T, "High Altitude Turbulence Detection using an Airborne Doppler Lidar", Proceedings of ICAS, St. Petersburg, Russia, (2014).

[12] Wilcox J. D. Isokinetic Flow and Sampling, *Journal of the Air Pollution Control Association*, 5:4, 226-245, 1956.

Copyright Statement